Macromolecules

Open Access
This article is licensed under CC-BY 4.0

pubs.acs.org/Macromolecules
Article

Amino-yne Reaction for the Synthesis of Degradable Hydrogels: Study of the Cleavage of β-Aminoacrylate Cross-Links

Sara Bescós-Ramo, Jesús del Barrio, Pilar Romero, Laura Florentino-Madiedo, Milagros Piñol,* and Luis Oriol*

Cite This: *Macromolecules* 2024, 57, 10926−10937
Read Online

ACCESS | Metrics & More | Article Recommendations | Supporting Information

ABSTRACT: This work addresses a study of PEG-derived hydrogels based on β-aminoacrylate cross-links and obtained by amino-yne click chemistry, using a β-aminoacrylate-based model molecule as reference. The pH-triggered cleavage of the β-aminoacrylate bonds was monitored confirming not only the release of the conjugated amine but also the formation of a mixture of chemical species that depends on the acidity of the medium. Moreover, overall hydrogel degradation rates were able to be adjusted by modifying pH, temperature, polymer concentration, or the amine selected as linker of PEG chains. In particular, the labile nature of the β-aminoacrylate bond was confirmed even under physiological conditions (pH 7.4, 37 °C), leading to long-term material degradation. The release and recovery of the conjugated amine after the cleavage of the β-aminoacrylate bonds was demonstrated at both acidic and physiological pH, mimicking the results acquired through model molecule studies.

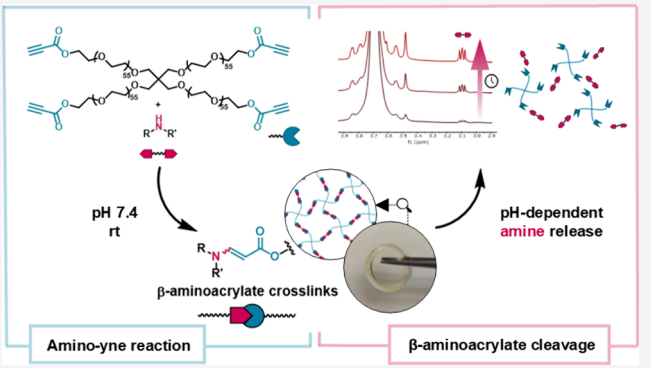

Downloaded via UNIV DE ZARAGOZA on January 31, 2025 at 09:15:21 (UTC).
See https://pubs.acs.org/sharingguidelines for options on how to legitimately share published articles.

INTRODUCTION

Hydrogels are attractive candidates for a variety of biomedical applications such as tissue engineering,[1] wound dressing,[2,3] and drug delivery.[4] In this context, while natural polymers can effectively replicate certain properties of physiological environments, synthetic polymers offer the possibility of tuning their mechanical characteristics and chemical composition. Among them, poly(ethylene glycol) (PEG)-based materials have demonstrated excellent biocompatibility and low toxicity.[5] The gelation process can be achieved through numerous mechanisms using either noncovalent (electrostatic interactions, hydrogen bonds) or covalent cross-linking.[6] Comparatively, chemically cross-linked hydrogels have proven superior mechanical strength than noncovalently cross-linked ones. Various chemical approaches have been employed to synthesize chemically cross-linked hydrogels under physiological conditions, with radical polymerizations being one of the commonly used methods. Nevertheless, recent attention has been drawn to hydrogels synthesized using click-like chemistries, especially metal-free ones, due to their high efficiency, selectivity, and ease of implementation, as well as their improved biocompatibility. These methodologies encompass a range of reactions, including but not limited to, the strain or electron-withdrawing group-promoted azide−alkyne [3 + 2] cycloaddition (SPAAC),[7−13] radical mediated and Michael addition thiol-ene,[14−17] Diels−Alder,[18,19] oxime-forming,[20−23] and nucleophilic additions to activated alkynes such as thiol-yne[24−27] or hydroxyl-yne reactions.[28] However, covalent bonds are mostly stable, which limits their potential applications in the biological field when degradable materials are desirable. Alternatively, cleavable covalent bonds provide the opportunity to engineer materials that degrade over time or in response to specific stimuli in a controlled way. The incorporation of these labile bonds into the polymer network enables the degradability of the hydrogel system, which is essential to prevent long-term accumulation of polymer remnants.[29,30] Moreover, by including stimuli-responsive cleavable groups into the cross-linking points, hydrogels can not only degrade but also enable the conjugation of drugs through these labile groups and provoke their release upon applying the stimulus, rather than simply diffusing if the drug is physically retained within the hydrogel.[31−33] To date, among the various stimuli employed to induce breakage of a covalent bond, pH-responsive hydrogels have been commonly prepared using a wide variety of acid-labile cross-linking agents such as hydrazones, imines, and acetals or ketals.[34−36]

Among the different chemistries, the outstanding amino-yne click reaction has gained recent interest in polymer science since

Received: June 17, 2024
Revised: October 8, 2024
Accepted: November 19, 2024
Published: November 28, 2024

© 2024 The Authors. Published by American Chemical Society

its initial report in 2017 by Tang's group.[37] This reaction can occur under click-like conditions, i.e. it proceeds spontaneously at room temperature and in aqueous media, by simply mixing amines (amino-) and electron-withdrawing alkynes (-yne). Additionally, the resultant β-aminoacrylate bond has been found to be cleavable under acidic conditions (pH < 5.5), allowing for the recovery of the initial amine and generation of 3-oxopropanoates.[38,39] Besides, bond breakage can be induced by the presence of singlet oxygen species ($^1O_2$) resulting in the generation of alcohols and *N*-formyl derivatives, instead of affording the amine.[40] Despite being a versatile click reaction, amino-yne chemistry has been scarcely applied to the preparation of hydrogels. Langer et al. reported the first amino-yne-based hydrogels using PEG tetra-alkynoates and water-soluble primary, secondary, and tertiary amines. Their study demonstrated that the latter were unable to induce gelation.[41] Huang and Jiang prepared chitosan and dipropiolate PEG hydrogels showing their pH-responsiveness.[42] Furthermore, the applicability of this chemistry has also been demonstrated in various hydrogel fields, including the preparation of corneal substitutes,[43] enzyme immobilization,[44] wound healing,[45,46] 3D printing,[47] cell scaffolds,[48] or light-degradable hydrogels mediated by singlet oxygen using a photosensitizer molecule,[49,50] among others.

To engineer a degradable hydrogel, it is crucial to have a deep understanding of the chemistry of the cleavable groups, their byproducts, and the factors defining the degradation rates.[51] However, despite the confirmed recovery of the initial amine-based molecule at approximately pH < 5.5,[39,52,53] there is a lack of literature addressing the chemistry underlying the cleavage of the β-aminoacrylate and products generated by the breakage of this bond. Therefore, in this work, a β-aminoacrylate-based model molecule was synthesized through spontaneous amino-yne reaction to investigate (i) the feasibility of amine release in aqueous media at different pH, from physiological to strongly acidic, and different temperatures and (ii) the chemical nature of other products resulting from the β-aminoacrylate cleavage under different conditions. Next, PEG tetra-alkynoate-based hydrogels were synthesized using a variety of multifunctional primary and secondary amines and different polymer concentrations, in order to get further insights and precise control over their effect on the stability of the network. After hydrogel characterization, pH- and temperature-triggered degradations were studied, underscoring relatively fast β-aminoacrylate cleavage under acidic media. Such a process also occurs under physiological conditions, although at a slower pace. The feasibility of transferring the gained knowledge from the model molecule to the hydrogels was established by comparing the resultant byproducts of the hydrogel degradation with those identified in the low-molecular-weight model compound.

RESULTS AND DISCUSSION

Formation and Cleavage of β-Aminoacrylate Bond in a Model Molecule. With the aim of studying the amino-yne click reaction in aqueous media and the responsive properties of the resulting β-aminoacrylate bond, the model compound **TEG$_2$-A1** (Figure 1a) was prepared. First, water-soluble propiolate **TEGalk** was synthesized by reacting tri(ethylene glycol) monomethyl ether with propiolic acid according to a Fischer esterification protocol.[54] Then, **TEG$_2$-A1** was obtained by mixing **TEGalk** and *N,N′*-dimethyl-1,3-propanediamine (**A1**, Figure 1a) in a 2:1 molar ratio at pH 7.4, in a 0.1 M phosphate buffer (PB). Complete conversion was observed after approximately 10 min at room temperature in the absence of a catalyst. As previously reported for similar secondary amines,[37] the reaction demonstrated *E*-selectivity yielding exclusively the *trans* isomer as evidenced by the proton nuclear magnetic resonance (^{1}H NMR) spectrum (Figure 1b, **TEG$_2$-A1** pH = 7.4).

Based on previous references proposing the acid pH-triggered cleavage of β-aminoacrylate bond into amine and 3-oxopropanoate species,[39,42] strong acidic conditions were chosen for an initial study of a fast evolution of the bond, followed by exploring the differences with moderate acidic conditions. **TEG$_2$-A1** was dissolved in aqueous solutions of different pH values (2.0 and 5.0) at 25 °C, and changes were monitored by recording ^{1}H NMR spectra at appropriate time intervals. Under pH 2.0, the enaminone protons disappeared completely in less than 10 min, accompanied by the emergence of the protonated amine signals, indicating the expected complete release of **A1** (Figure 1b). However, the initially anticipated product 3-oxopropanoate (**1** in Figure 1a) was not detected. Instead, two new signals at 5.40 and 2.65 ppm appeared that could be assigned to the resonances of the C=CH (*i*) and CH$_2$ (*j*) groups, respectively, of the product resulting from an acid-catalyzed aldol condensation (**2** in Figure 1a). This was confirmed by their correlation shown by the homonuclear correlation spectroscopy (COSY) experiment (Figure S7) and supported by the electrospray ionization (ESI) mass spectrometry experiment (Figure S8), which revealed a main peak (m/z = 474, (+Na)) that corresponds to the sodiated molecular species of the α,β-unsaturated aldehyde adduct.

When **TEG$_2$-A1** was dissolved in a moderately acidic buffer (pH = 5.0), a slowdown in the cleavage of the enamine bond was observed, and 24 h was required for almost complete disappearance of the corresponding ^{1}H NMR signals (Figure 2b). Protons of the released **A1** emerged concurrently with those of the species in which only one of the =C−N− bonds was broken (**TEG-A1** in Figure 2a and protons labeled as *c′* and *d′*). Additionally, different products arising from the cleavage of the β-aminoacrylate bond were also identified. Initially, a triplet at 5.40 ppm assigned to the aldehyde adduct **2** (labeled as *i*) appeared but, after 1 h, it turned into a new set of signals not detected when degradation was undertaken at pH = 2.0. Besides, two major singlets were observed downfield at 8.83 and 8.44 ppm. The former was associated with the ester of the benzene-1,3,5-tricarboxylic acid (**3** in Figure 2a) according to the ^{1}H−^{13}C heteronuclear single-quantum correlation (HSQC) (correlation with ^{13}C signal at δ = 137.3 ppm, Figures S12 and S13) and the main peak in the ESI-MS experiment (Figure S10, m/z = 671 (+Na)). The formation of this derivative (**3**) was fully confirmed by the ^{1}H−^{13}C heteronuclear multiple bond correlation (HMBC) spectrum (Figures S14 and S15). As previously described, this aromatic derivative results from the cyclotrimerization of enaminones in acidic conditions,[55,56] specifically using sodium acetate and acetic acid as catalyst and solvent,[57] respectively, which are components of the buffer used at pH = 5.0 in this study. However, this species was also observed when employing a pH 5.0 sodium citrate/citric acid buffer (Figure S17), suggesting that its formation could be considered a more generalized process rather than being solely a consequence of the buffer composition. The peak at δ = 8.44 ppm was assigned to an aldehyde-type species, according to its HSQC correlation with a ^{13}C signal at δ = 173.6 ppm (Figures S12 and S13). The formation of oxopropanoate **1** was also observed, not as the isolated species but as a cyclic trimer

https://doi.org/10.1021/acs.macromol.4c01403
Macromolecules 2024, 57, 10926−10937

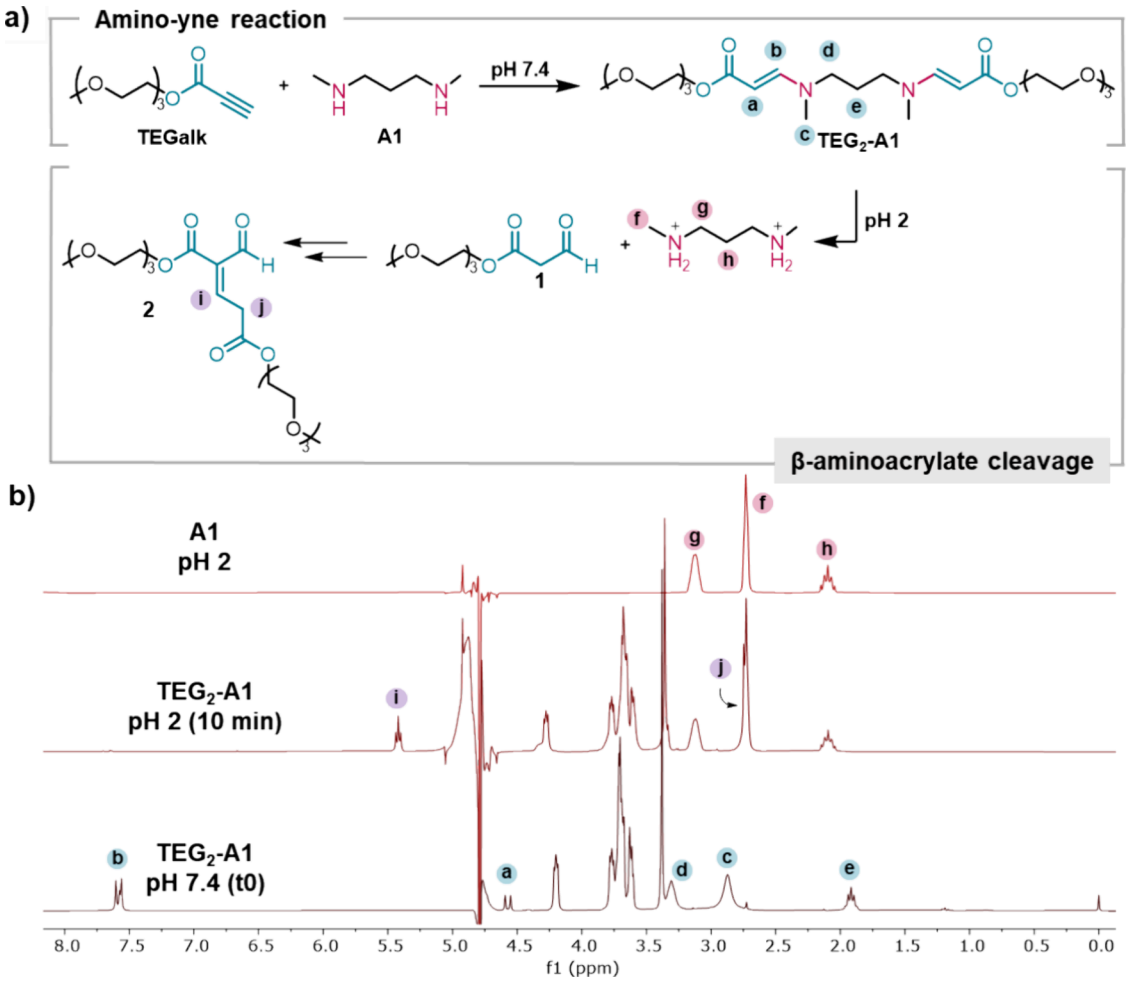

Figure 1. (a) Scheme of amino-yne click reaction and β-aminoacrylate cleavage at pH = 2.0 and 25 °C; (b) from bottom to top: water-suppressed ^{1}H NMR spectra of **TEG$_2$-A1** at pH = 7.4 (pH = 7.4, buffer/D$_2$O 9:1, 300 MHz), after 10 min at pH = 2.0 (pH = 2.0, aqueous solution/D$_2$O 9:1) and **A1** at pH = 2.0, as reference.

resulting from its condensation equilibrium in this acidic medium. This resulting 1,3,5-trioxane derivative was identified by HSQC and HMBC correlations (Figures S12 and S14) as well as by ESI-MS (Figure S10, m/z = 725 (+Na)). Although the characterized species do not disclose the complete mixture of the overall degradation products, these results reveal that the β-aminoacrylate cleavage is a more complex process than previously reported in literature, involving the evolution of the initially resultant aldehyde, or even side reactions of β-aminoacrylates depending on the pH. Nonetheless, the release of the amine is complete and firmly established, with its release rate highly dependent on the pH of the medium.

The evolution of **TEG$_2$-A1** at pH 7.4 and 25 °C was also investigated. Surprisingly, after 1 h, new signals appeared at the upfield part of the spectrum (labeled as *c'* and *d'* in Figure 2c). They seemed to correspond, again, to the species in which only one of the =C−N− bonds was broken (**TEG-A1**). After 4 h, the amine **A1** signals were also detected. Additionally, aldehyde and aromatic proton singlets appeared in the downfield as minor compounds. By recording a diffusion-ordered spectroscopy (DOSY) experiment after 24 h, at least three different species were identified according to their diffusion coefficients (Figure S18). The smallest diffusion coefficient corresponds to **TEG$_2$-A1**, the highest to **A1**, and the intermediate one matches **TEG-A1**.

Finally, changes of **TEG$_2$-A1** at pH 7.4 and pH 5.0 were also monitored at 37 °C, to assess a possible acceleration of β-aminoacrylate cleavage at physiological temperature. In both cases, temperature accelerates the disappearance of the β-aminoacrylate bond, but its effect was far less pronounced than that of lowering the pH, at least within the first 48 h (Figure S19). Bond cleavage gave rise to the already described products, and no signals of ester hydrolysis were detected in the spectra. In conclusion, at physiological pH, the β-aminoacrylate bond has a much greater stability than in an acid medium, but a slow cleavage of the bond ultimately resulting in the release of the amine is still observed.

Synthesis and Characterization of Hydrogels. The synthesis of hydrogels was accomplished using a propiolate-functionalized four-armed poly(ethylene glycol) and different commercially available aliphatic amines. To this end, PEG tetra-alkynoate (**PEGalk**) with average molecular weight of 10,000 g mol^{-1} was first synthesized following a previously reported protocol (Figure S20).[41] Complete functionalization was corroborated by ^{1}H NMR spectroscopy, and further characterization was accomplished by Fourier transform infrared spectroscopy (FTIR), matrix-assisted laser desorption/ionization-time-of-flight (MALDI-ToF) mass spectroscopy, and differential scanning calorimetry (DSC) (Figures S21−S24).

https://doi.org/10.1021/acs.macromol.4c01403
Macromolecules 2024, 57, 10926−10937

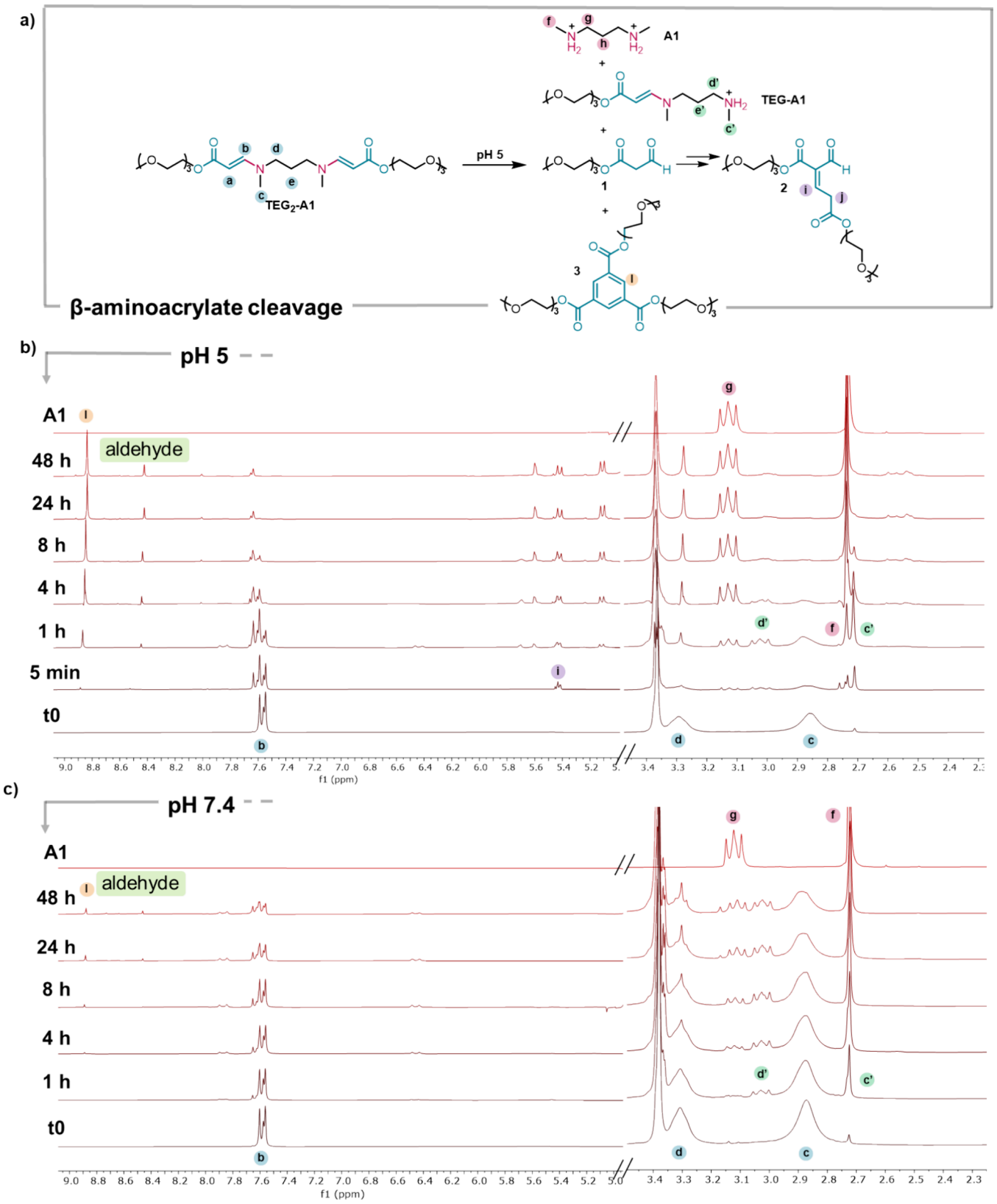

Figure 2. *β*-Aminoacrylate cleavage at 25 °C: (a) scheme of **TEG_2-A1** degradation products at pH 5.0; (b) water-suppressed ^{1}H NMR spectra at pH = 5.0 at different time intervals (pH = 5.0 buffer/D_2O 9:1, 300 MHz); (c) water-suppressed ^{1}H NMR spectra at pH = 7.4 at different time intervals (pH = 7.4 buffer/D_2O 9:1, 300 MHz). Amine **A1** appears as the protonated species in all cases.

For the preparation of the hydrogels, **PEGalk** was weighted according to the desired polymer concentration (wt %) in the final hydrogel and dissolved in a pH = 7.4 buffer by orbital mixing overnight. Amine, which provokes macromolecular network formation, was separately dissolved in the same buffer. Both solutions were mixed, ensuring a 1:1 molar ratio of amine

https://doi.org/10.1021/acs.macromol.4c01403
Macromolecules 2024, 57, 10926−10937

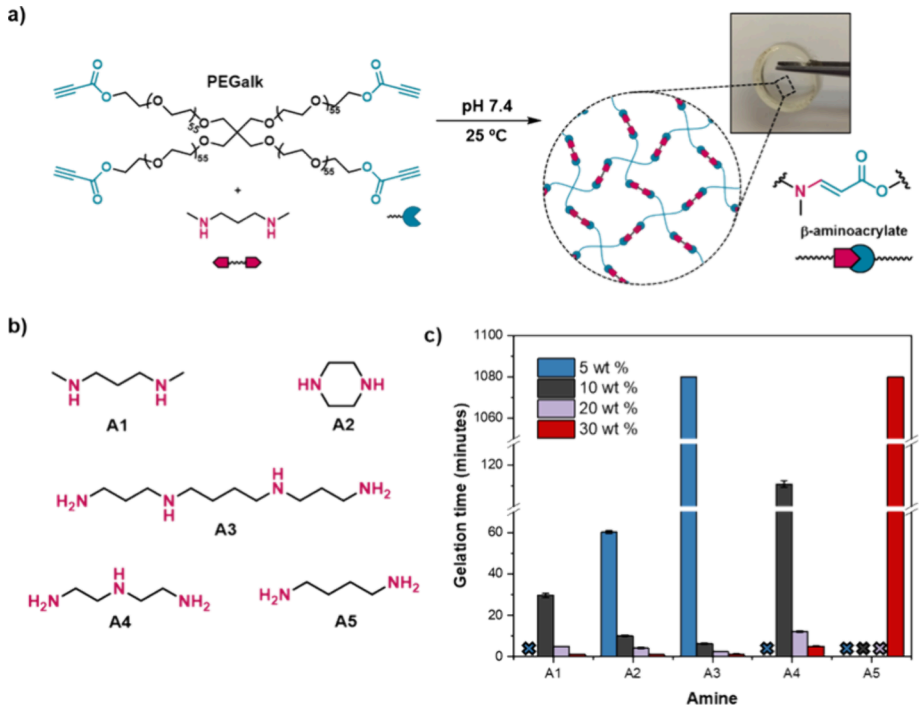

Figure 3. (a) Depiction of hydrogel formation from **PEGalk** and **A1** at pH 7.4 and 25 °C resulting in a self-standing transparent yellowish material (right); (b) chemical structure of the different amines investigated for the network formation and (c) gelation time by inverted vial test at 25 °C depending on the polymer concentration and cross-linker (data presented as mean ± SD (n = 3)). Crosses indicate no gelation was recorded after 24 h.

vs alkynoate groups and a final mass of 200 mg of the resulting hydrogel in all cases. After 10 s of vortex mixing, hydrogels were allowed to set at 25 °C (for a more detailed procedure, see Experimental Section and Table S1). Once gelation was completed, a self-standing yellowish material was obtained, as shown in Figure 3a, where difunctional amine **A1** is used as an example to illustrate network formation.

The synthesis of hydrogels was studied by varying polymer concentration (5, 10, 20, and 30 wt %) and amine functionality. For the latter, five multifunctional primary and secondary amines were used: *N,N'*-dimethyl-1,3-propanediamine (**A1**), piperazine (**A2**), spermine (**A3**), diethylenetriamine (**A4**), and 1,4-diaminobutane (**A5**) (Figure 3b). Then, qualitative determination of gelation time was carried out by the inverted vial test. Various trends can be extracted from the results summarized in Figure 3c. First, gelation time could be tuned by varying the polymer weight percentage. As a result of increasing the concentration of reactive groups in the final mixture, higher polymer wt % led shorter gelation times for the same cross-linker. Second, taking into account cross-linkers with the same number of amine groups, **A1**, **A2**, and **A5**, gelation time decreased with increasing nucleophilicity of the amine. Whereas the cyclic secondary amines induced network formation faster than the linear ones ($t_{gelA2} < t_{gelA1}$), gelation proceeded slower for primary amines ($t_{gelA1} < t_{gelA5}$). Therefore, **A5** only formed hydrogels overnight at 30 wt %, whereas all other gels were obtained at 10 wt % (**A1** and **A4**) or even at 5 wt % (**A2** and **A3**) polymer concentration. Finally, by increasing the number of cross-linking points, gelation was also accelerated. For instance, **A4**, which has two primary and one secondary amine groups, formed hydrogels faster and at a lower polymer concentration than **A5**, with only two primary amines. The biobased spermine, **A3**, which has the highest number of cross-linking points, induced the fastest gelation among all linear amines, and only **A2** cross-linked faster at 5 wt % polymer concentration.

Preliminary rheological studies were performed to follow the kinetics of network formation at pH 7.4, using **PEGalk-A1** hydrogel as example (see Experimental Section, Rheological measurements). For that purpose, the evolution of the storage (G') and loss (G'') moduli of the hydrogel (10 wt % polymer concentration) with time was monitored at 25 °C (Figure 4a). The material was left to gel for 24 h to ensure the maximum possible cross-link density, observing two different regions in our time sweeps. Initially, G' exhibited a sharp increase, where G' surpassed G'' only 6 min after lowering the upper plate, to then steadily grow until it reached a maximum at approximately 7 h. Subsequently, the storage modulus began to decrease, presumably due to some kind of network degradation over time (*vide infra*). Experiments were replicated at 37 and 15 °C, revealing a temperature-dependent degradation boosted at the physiological temperature (Figures S26 and S27). It was observed that the decline of G' at a higher temperature (37 °C) initiated at earlier times and also dropped to a larger extent in comparison to samples evaluated at 15 °C. Indeed, G' remained stable when the time sweep was recorded at a temperature below rt. In these time sweep experiments, the maximum G' value for the 30 wt % hydrogel was higher than that for the 10 wt % hydrogel (ca. 8.9 and 0.7 kPa for 30 and 10 wt %, respectively). However, as previously discussed, G' decreases after reaching its maximum, with this decline being more pronounced in the 30 wt % hydrogel compared to the 10 wt % hydrogel (Figure S28). This decay in G' might be associated with polymer network degradations.

Encouraged by the apparent loss of network integrity over time even at 25 °C, the structural characterization of 10 wt % hydrogel was performed 24 h after mixing the precursor solutions by high-resolution magic angle spinning (HR-MAS)

https://doi.org/10.1021/acs.macromol.4c01403
Macromolecules 2024, 57, 10926−10937

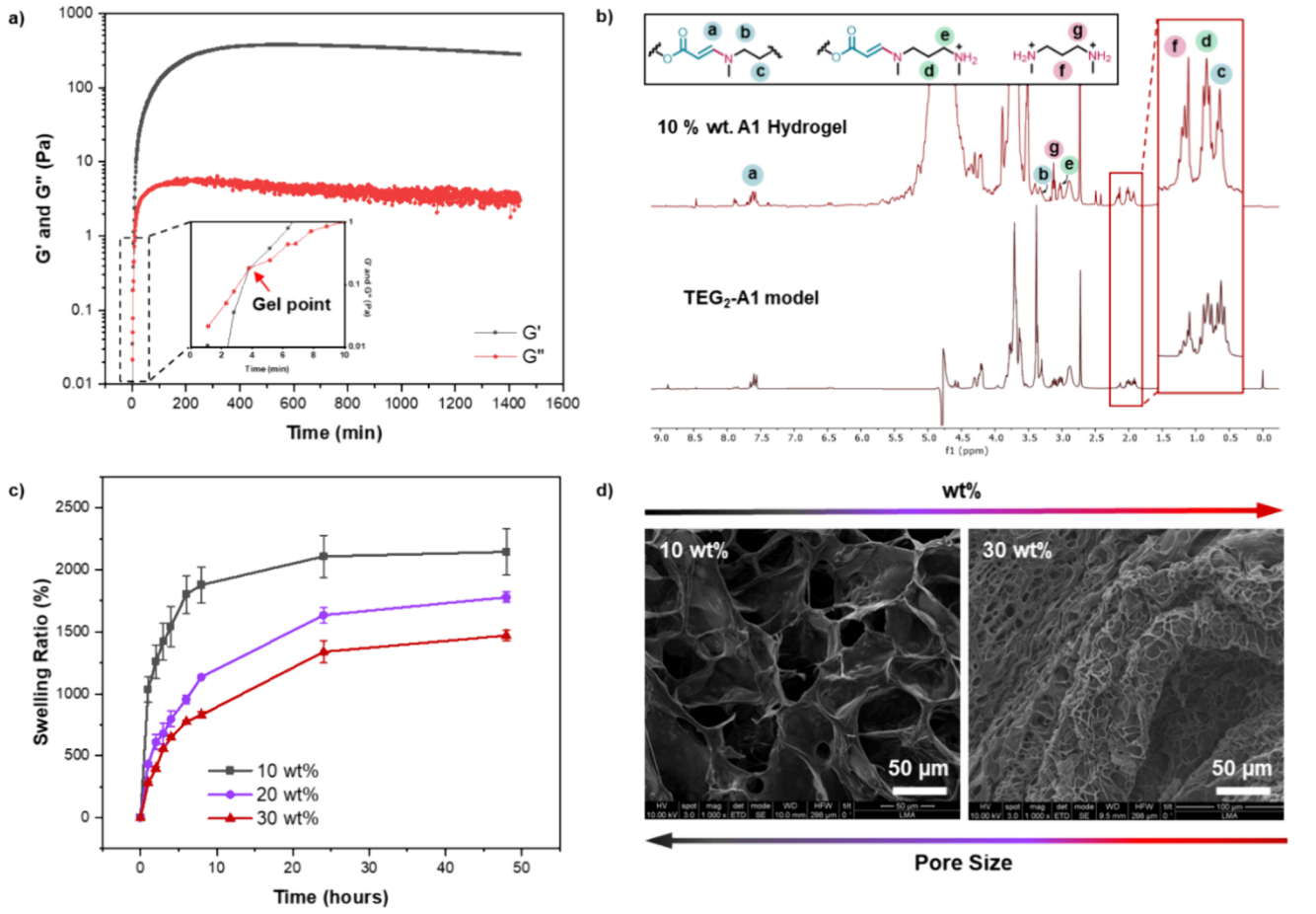

Figure 4. (a) Evolution of storage (G') and loss (G'') moduli as a function of time at 25 °C for 10 wt % **PEGalk-A1** hydrogel. Gelation time is pointed out by the crossover point between G' and G''. (b) ^{1}H-HR-MAS NMR spectrum of 10 wt % **PEGalk-A1** hydrogel 24 h after mixing both **PEGalk** and **A1** at pH = 7.4 (a drop of D_2O was added before starting the experiment, 400 MHz, up) and water-suppressed ^{1}H NMR of **TEG$_2$-A1** model molecule after 24 h at pH = 7.4 (pH = 7.4 buffer/D_2O 9:1, 300 MHz, down as reference). (c) Swelling behavior of **PEGalk-A1** hydrogels varying polymer concentration (data was presented as mean ± SD (n = 3)) and (d) SEM image of the cross-sectional morphology of **PEGalk-A1** swollen hydrogels 10 wt % (left) and 30 wt % (right).

NMR spectroscopy. As seen in Figure 4b, a mixture of β-aminoacrylate (signals labeled as *a*, *b*, and *c*), partially broken species (signals labeled *d*, *e*), and free amine (signals labeled *f*, *g*) were clearly observed in the hydrogel matrix. Hence, the emergence of these signals and the decrease in G' over time at pH 7.4 could be elucidated by the partial cleavage of β-aminoacrylate (as proposed with the model molecule) prior to or just after the complete formation of the hydrogel, with both processes likely occurring simultaneously after a certain time.

We then moved to the macroscopic characterization of hydrogels in order to quantify their water permeability. Accordingly, their swelling ratio, i.e., the relative weight increase of the hydrogel due to water absorption,[58] and equilibrium water content (EWC), which indicates the water content of the hydrogel in a steady state, were calculated at pH = 7.4 and a fixed temperature (25 °C). As shown in Figure 4c, **PEGalk-A1** hydrogels at 10, 20, and 30 wt % were able to rapidly absorb water, reaching their equilibrium state after 24 h with high EWC percentages (>94%). When comparing the swelling ratios of 10, 20, and 30 wt % hydrogels (approximately 2100, 1650, and 1350, respectively), it was highlighted that the increase in polymer concentration led to a decrease in water uptake. These findings also matched with the high porosity of the materials, as well as with the trend in porous size, exposed while observing the cross-section of swelled and freeze-dried hydrogels by scanning electron microscopy (SEM, Figure 4d) and the results of mercury intrusion porosimetry (MIP, Figures S29−S31). Their morphology characterization revealed a highly porous structure, for which the porous size decreased as polymer concentration increased (Figure 4d). MIP allowed us to evaluate the macroporosity (>50 nm) and mesoporosity (50−2 nm) of **PEGalk-A1** swollen hydrogels of 10, 20, and 30 wt % in detail. The results clearly indicate that the hydrogels were predominantly macroporous (97−99% of total pore volume, Table S2). 10 and 20 wt % hydrogels presented quite a bit of variability in their replicas, resulting in the same average pore volume value (2.1 mL/g). However, when using 30 wt %, the replicates exhibited very similar porosity, and the difference compared to the lower percentages was clear, with the volume being reduced by half (1.0 mL/g). Therefore, an increase in the polymer concentration resulted in a smaller pore size and, consequently, lower swelling. This might be a consequence of an increase in the number of physical chain entanglements formed when polymer concentration increased, as previously reported.[59] Since disentanglement of polymeric chains does not occur completely with swelling experiments, swelling ratio includes the effect of both chemical cross-linking and physical entanglements.[59−61]

https://doi.org/10.1021/acs.macromol.4c01403
Macromolecules 2024, 57, 10926−10937

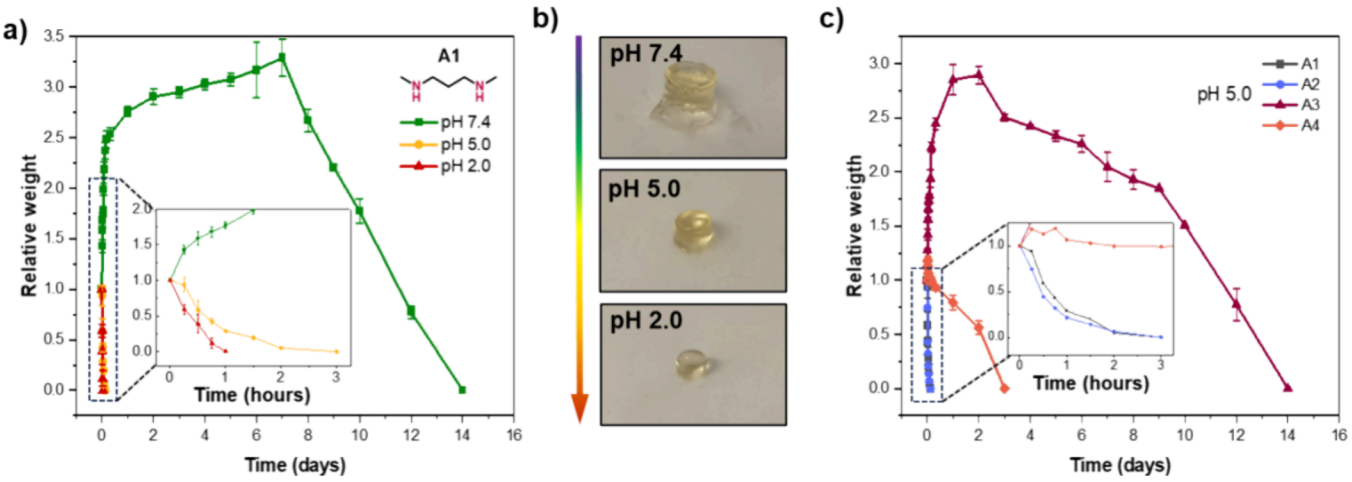

Figure 5. pH-induced degradation behavior at 25 °C. (a) Relative weight over time of 10 wt % **PEGalk-A1** hydrogels immersed at pH = 7.4, 5.0, and 2.0 at 25 °C; (b) images of 10 wt % **PEGalk-A1** hydrogels (with same initial shape and weight) after 30 min immersed at different pH (all three images were taken in the same scale; see Figure S34); (c) relative weight over time of 10 wt % **PEGalk-A1/2/3/4** hydrogels at pH = 5.0.

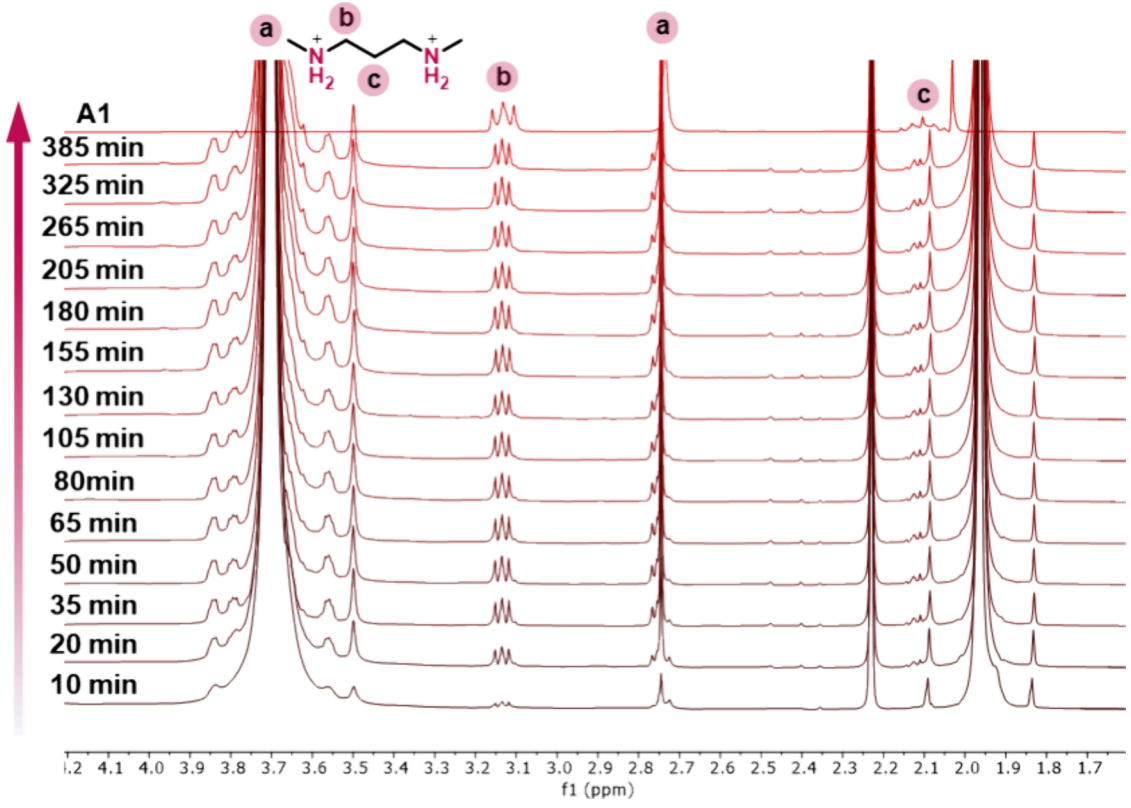

Figure 6. Water-suppressed ^{1}H NMR spectra over time of 10 wt % **PEGalk-A1**'s solubilized degradation products (pH = 5.0 buffer/D_2O 9:1, 500 MHz). The spectrum of **A1** is included as a reference.

Furthermore, the contribution of the degradation over time observed during rheological experiments cannot be dismissed.

Hydrogel Degradation. Concerning the pH-responsiveness of the hydrogel, network degradation rate was studied by immersing freshly prepared 10 wt % **PEGalk-A1** hydrogels (total mass of hydrogel approximately 200 mg) into 2 mL of the aqueous solutions at different pH (2.0, 5.0, and 7.4) at 25 °C and weighting them over time (see details in Experimental Section). Their relative weight was monitored as an indirect measure of their degradation associated with mass loss and the formation of soluble species in the media. In Figure 5a, it is observed that pH = 2.0 led to fast erosion of the material and its solubilization after 1 h, which can be mainly attributed to the breakage of β-aminoacrylate cross-links of the network. With model molecule studies, it was demonstrated that strong acidic conditions induce rapid β-aminoacrylate cleavage, whereas pH 5.0 led to a more gradual cleavage with emergence of free amines. In the case of the hydrogels, a moderately acidic medium, pH = 5.0, appeared to facilitate network degradation leading to soluble species after 3 h, while at pH = 7.4, relative weight only started to decrease after the 8th day, and complete solubilization was not detected before the 14th day. Macroscopically, the acidic pH resulted in

https://doi.org/10.1021/acs.macromol.4c01403
Macromolecules 2024, 57, 10926−10937

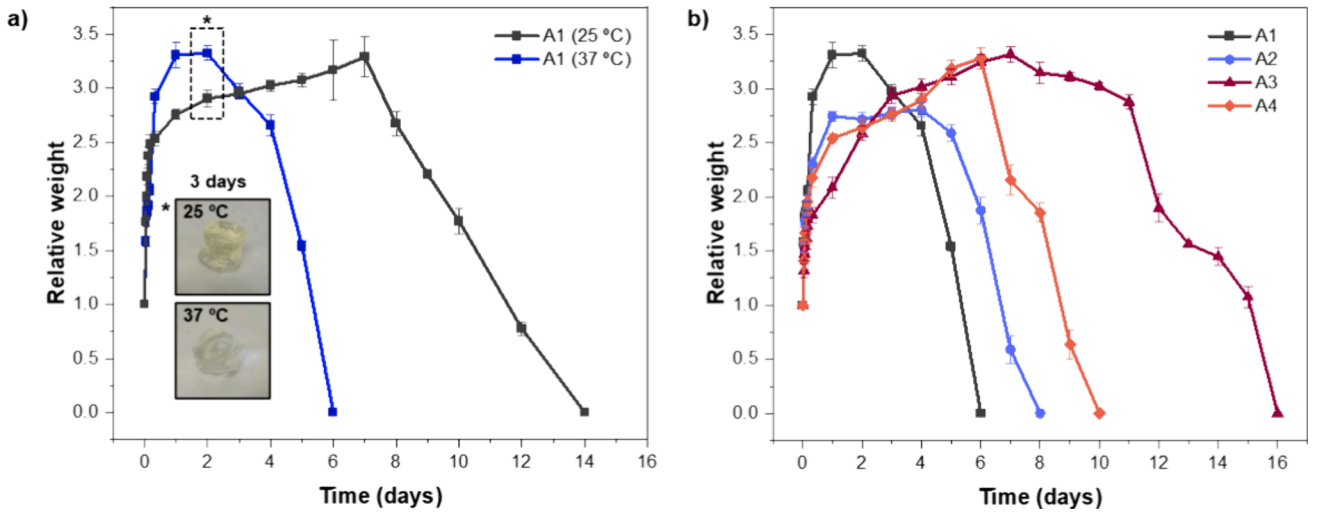

Figure 7. (a) Temperature-induced degradation behavior over time of 10 wt % **PEGalk-A1** hydrogels at 25 and 37 °C and (b) 10 wt % **PEGalk-A1/2/3/4** hydrogels at 37 °C.

progressive erosion of the hydrogel, which decreased in weight and size over time and more rapidly as the pH became more acidic (Figure 5b).

In order to check the influence of the cross-linker on the network degradation rate, experiments were replicated with 10 wt % **PEGalk-A2/3/4**, using the other three different amines that proved to gel at the selected polymer concentration (10 wt %). When comparing degradation rates of the hydrogels at 25 °C, the same trend was observed independently of the pH (Figure S32 for pH = 2.0 and 7.4, Figure 5c for pH = 5.0). Whereas **PEGalk-A1** and **PEGalk-A2** behaved similarly, hydrogels prepared with **A3** and **A4** exhibited a retarded decrease in their relative weight, likely attributed to their higher number of theoretical cross-link points, which creates more dense networks that are less prone to degradation. **PEGalk-A3** had significantly longer lifetime under acidic conditions, since weight loss was not registered before 8 h and the 4th day at pH = 2.0 and 5.0, respectively. 1 and 14 days were needed for their complete solubilization, compared to the hours-scale degradation of both **PEGalk-A1** and **PEGalk-A2**. For a more concentrated hydrogel, 30 wt % **PEGalk-A1**, similar results were obtained when compared with that of 10 wt % (Figure S33), so that polymer concentration does not seem to induce a big change on pH-responsive properties.

Recovery of the amine used as cross-linker after the hydrogel network degradation at acidic pH was also studied in aqueous solution. In order to do that, a small piece of 10 wt % **PEGalk-A1** hydrogel was introduced in an NMR tube and immersed in 9:1 (v/v) solution of pH = 5.0 buffer and D_2O. ^1H NMR spectra, which correspond to degradation products solubilized in aqueous media, were collected over time. Clear signals of amine **A1** were observed, as highlighted in Figure 6. The integration of amine protons gradually increased, revealing its progressive release, until signals seem to maintain their intensity approximately after 3 h. Additionally, the downfield part of the spectra revealed the apparition of the signals assigned to the β-aminoacrylate cleavage species already characterized on the model molecule studies (Figure S35).

The effect of temperature on β-aminoacrylate hydrogel stability was studied by comparing their swelling and degradation at pH 7.4 at two different temperatures: 25 and 37 °C. Therefore, 10 wt % **PEGalk-A1** hydrogels were immersed in the buffer at the selected temperature and, again, weighted over time. As observed in Figure 7a, the material initially underwent a weight increase as a result of water uptake at both temperatures. However, after 2−3 days, clear signs of hydrogel erosion such as rounded edges were shown for those at 37 °C. The material suffered a continuous decrease in weight that led to complete solubilization after 6 days, whereas for those immersed at 25 °C, collapse did not occur until the 14th day. With the aim to know the structural changes behind the degradation of the hydrogel at 37 °C, ^1H NMR spectrum of the fully solubilized hydrogel was recorded after freeze-drying the final resulting aqueous solution (Figure S36). First, signals of the protonated amine were observed, confirming that although β-aminoacrylate cleavage is significantly slowed down, it occurs even at physiological pH as previously demonstrated on the model molecule studies and HR-MAS NMR spectroscopy of the hydrogel. Furthermore, alpha protons of the ester group were not detected in the spectrum, suggesting that complete solubilization is also accompanied by ester hydrolysis at long degradation times. β-Aminoester-based molecules resulting from Michael addition of amines to acrylates have been proved to be hydrolytically labile at neutral or basic-like pH, even within hour scale.[62] However, ester hydrolysis seems not to be as favored in our case, probably because of the higher electron density on the acyl carbon of the ester bond provided by the double bond. Since ester hydrolysis was not detected in the degradation studies of the model molecule for up to 48 h, it is suggested that it occurs preferentially over extended periods of time, possibly spanning several days according to the results on the hydrogels.

Swelling/degradation experiments were also undertaken for 10 wt % **PEGalk-A2/A3/A4** at pH = 7.4 and 37 °C (Figure 7b). As expected, they reproduced the trend observed at 25 °C, so a higher cross-linking density seems to favor a stronger stability (**A3** > **A4** > **A2/1**). Therefore, hydrogels that were robust toward pH-triggered cleavage were also more resistant against the action of temperature. Regarding the effect of using a cyclic amine as piperazine (**PEGalk-A2**), it was noticed that the water uptake was lower than for **PEGalk-A1**, probably due to the higher rigidity of the network, which retards aminoacrylate cleavage and hydrolysis. In the case of **PEGalk-A3**, being the most stable hydrogel, relative weight started to decrease after the

https://doi.org/10.1021/acs.macromol.4c01403
Macromolecules 2024, 57, 10926−10937

9th day and complete breaking down of the material occurred beyond the 16th day. For **PEGalk-A1**, **A2**, and **A4**, complete solubilization of the hydrogel was detected at the 6th, 8th, and 10th days, respectively.

CONCLUSIONS

This work provides a deep insight into the degradation of hydrogels based on β-aminoacrylate cross-links. Studies have been conducted on a model bis(β-aminoacrylate) molecule to improve our understanding of the chemistry underlying the recovery of the initial amine after the cleavage of the bond. It should be underscored that contrary to previous assumptions, the pH-triggered cleavage of β-aminoacrylate not only yields 3-oxopropanoates but also different species are detected depending on the pH. Furthermore, it has been demonstrated that the β-aminoacrylate bond is also cleavable at physiological pH. Even though dissociation of the bond is slower compared to more acidic environments, it still results in a slow release of the amine. Regarding the hydrogels, they have shown a high-water-uptake capacity that makes them attractive candidates for biomedical applications such as wound dressing. Rheological measurements combined with HR-MAS NMR spectroscopy have revealed the dynamic nature of the β-aminoacrylate bond within the hydrogels even at physiological pH, as well as the significant differences in the final properties of the material induced by small changes in temperature (25 to 37 °C). The tunability of their degradation rates once the hydrogel is prepared has been proven to strongly depend on the cross-link density, as well as external changes on pH and temperature of the media. Finally, release of the conjugated amine after the pH-induced cleavage of the β-aminoacrylate bonds was demonstrated, mimicking results acquired through model molecule studies. This proof of concept paves the way to the use of amino-yne click reaction for conjugation and release of amino-based drugs, mediated by cleavage of β-aminoacrylate links inside of our hydrogel's network with a tunable degradability.

EXPERIMENTAL SECTION

Materials. Triethylene glycol monomethyl eter, propiolic acid, *N,N'*-dimethyl-1,3-propanediamine, piperazine, spermine, diethylenetriamine, 1,4-diaminobutane, and 3-(trimethylsilyl)propionic-2,2,3,3-d_4 acid sodium salt (TMSP) were purchased from Sigma-Aldrich and used without purification. 4-arm poly(ethylene glycol) (pentaerythritol as core) with a molar mass of 10,000 g mol^{-1} was purchased from JenKem Technology (Tianjin). Phosphate buffer (PB, 0.1 M, pH 7.4) was prepared by mixing 50 vol % of sodium phosphate dibasic heptahydrate solution (72 mM) and 50 vol % sodium phosphate monobasic monohydrate solution (28 mM) in Milli-Q water. Acetate buffer (0.1 M, pH 5) was prepared by mixing 50 vol % of 70 mM sodium acetate solution and 50 vol % of 30 mM acetic acid solution in Milli-Q water. An aqueous solution at pH 2.0 (0.1 M) was prepared by mixing appropriate amounts of potassium chloride (0.1 M) and hydrochloric acid (0.02 M) in Milli-Q water.

Characterization. ^{1}H NMR and ^{13}C NMR spectra were acquired on a Bruker Avance NEO 400 spectrometer if not detailed in the specific method. The experiments were performed at room temperature in different deuterated solvents ($CDCl_3$ or D_2O). FTIR spectra were recorded on a Bruker Vertex 70 FTIR spectrometer. The samples were prepared on KBr pellets with a concentration of the product of 1−2% (w/w). MALDI-TOF mass spectrometry was performed on an Autoflex Bruker mass spectrometer with a dithranol matrix. Positive and negative ion electrospray ionization high resolution (ESI HRMS) was performed on a Bruker Q-TOF-MS instrument in positive or negative ESI mode. Thermal analysis was performed by differential scanning calorimetry with DSC TA Instruments Q2000 at 10 °C min^{-1} scan rate. The sample was sealed in aluminum hermetic pans.

Synthesis. *Synthesis of **TEGalk**.* Triethylene glycol monomethyl ether (3.22 g, 19.39 mmol) was dissolved in toluene (50 mL). To this solution were added both propiolic acid (2.70 g, 38.58 mmol) and *para*-toluenesulfonic acid (184 mg, 0.97 mmol), and the mixture was allowed to reflux for 18 h using a Dean−Stark apparatus to remove water and drive the reaction to completion. The reaction was cooled to room temperature and then evaporated to dryness. The residue was purified by flash column chromatography on silica gel, initially eluting with hexane/ethyl acetate (8:2), gradually increasing the polarity to finish with a (1:1) mixture. The target compound was obtained as a yellow oil. Yield: 78%. ^{1}H NMR ($CDCl_3$, 400 MHz) δ (ppm): 4.33 (2*H*, t, J = 4.8 Hz), 3.74−3.54 (10*H*, m), 3.38 (3*H*, s), 2.90 (1*H*, s). ^{13}C NMR ($CDCl_3$, 100 MHz) δ (ppm): 152.8, 75.3, 72.1, 70.9, 70.8, 70.7, 68.8, 65.4, 59.2. FTIR (KBr) υ (cm^{-1}): 3340−3120 (Csp-H), 3020−2740 (Csp3-H), 2115 (C≡C), 1717 (C═O).

*Syntheis of **TEG2-A1**.* A solution of *N,N'*-dimethyl-1,3-propanediamine (244 mg, 2.32 mmol) in PB (2.5 mL) was added dropwise to the **TEGalk** (1 g, 4.64 mmol) solution in PB (2.5 mL). After stirring for 10 min, the aqueous solution was extracted with ethyl acetate (3 × 15 mL) and the organic fraction was dried over $MgSO_4$ and evaporated to dryness. The compound was obtained as a yellow oil. Yield: 82%. ^{1}H NMR ($CDCl_3$, 400 MHz) δ (ppm): 7.57 (2*H*, *d*, J = 12.8 Hz), 4.56 (2*H*, *d*, J = 12.8 Hz), 4.19 (4*H*, *t*, J = 4.8 Hz), 3.77−3.59 (20*H*, m), 3.37, (6*H*, s), 3.30 (4*H*, *t*, J = 7.2 Hz), 2.86 (6*H*, s), 1.91 (2*H*, quint, J = 7.2 Hz). ^{13}C NMR ($CDCl_3$, 100 MHz,) δ (ppm): 169.3, 152.1, 84.9, 71.9, 70.6, 70.5, 70.5, 69.8, 62.3, 59.1. FTIR (KBr) υ (cm^{-1}): 3708−3217 (Csp2-H), 3072−3760 (Csp3-H), 1687 (C═O), 1614 (C═C).

*Synthesis of **PEGalk**.* 4-arm poly(ethylene glycol) (HO-ended) (1.50 g, 0.15 mmol) was dissolved in toluene (25 mL). Propiolic acid (422 mg, 6.00 mmol) and *para*-toluenesulfonic acid (37.1 mg, 0.20 mmol) were added, and the mixture was allowed to reflux for 48 h using a Dean−Stark apparatus to remove water and drive the reaction to completion. After cooling down the reaction to room temperature, the mixture was evaporated to dryness. The resultant residue was dissolved in dichloromethane and precipitated in ice-cold diethyl ether three times (3 × 200 mL), isolating the product by filtration. The final compound was dried under vacuum overnight, obtaining a white powder. It was observed that after storing the product at room temperature for several weeks, it eventually became insoluble in water as well as in other common organic solvents. Therefore, it should be stored in the refrigerator under argon. Under these storing conditions, the final compound can be safely handled at room temperature during a few days before observing any side reaction. Yield: 90%. ^{1}H NMR ($CDCl_3$, 400 MHz) δ (ppm): 4.34 (8*H*, *t*, J = 4.8 Hz), 3.75−3.52 (896*H*, m), 3.40 (8*H*, s), 2.96 (4*H*, s). FTIR (KBr) υ_{max}, (cm^{-1}): 3220 (Csp-H), 2889 (Csp^3−H), 2112 (Csp-Csp), 1715 (C═O).

Model Molecule NMR Study of the pH-Induced β-Aminoacrylate Cleavage. **TEG_2-A1** was dissolved in an aqueous solution of the appropriate pH (7.4, 5.0 or 2.0) in a concentration of 0.06 M. Aliquots of 450 μL were diluted with 50 μL of D_2O (TMSP was used as internal standard in the deuterated solvent at 1 mg mL^{-1} concentration) and transferred into an NMR tube. ^{1}H NMR spectra were collected over time. pH was adjusted when needed with 1 M HCl. Monodimensional NMR spectra were recorded at room temperature in a Bruker Avance III 300 MHz spectrometer equipped with a BBOF probe and applying a NOE water suppression experiment. Bidimensional experiments were acquired on a Bruker Avance NEO 400 spectrometer. Chemical shifts are given in parts per million relative to the TMSP internal standard.

Hydrogel Preparation. Hydrogels were prepared in 1.5 mL glass vials (8 × 35 mm) with a final mass of 200 mg (**PEGalk** + solvent), assuming the pH 7.4 buffer density is approximately 1 g/mL and dismissing the amine's mass. First, an appropriate amount of **PEGalk** was weighted in the glass vial to achieve polymer concentrations of 5, 10, 20, or 30 wt % in the final mass. Then, it was dissolved in 75% of final volume of pH 7.4 buffer used by orbital mixing overnight. **PEGalk** ^{1}H NMR spectrum was collected after 24 h of being dissolved in pH = 7.4 buffer in order to verify that no side reactions occur before hydrogel

https://doi.org/10.1021/acs.macromol.4c01403
Macromolecules 2024, 57, 10926−10937

preparation (Figure S25). The amine solution in the pH 7.4 buffer was prepared so that a 1:1 stoichiometric ratio of amine group:alkynoate is reached after adding the cross-linker in 25% of the final volume of the buffer. After 10 s of vortex mixing, hydrogels were allowed to set at a controlled temperature of 25 °C for 24 h. Table S1 exemplifies the mass, volume, and concentrations used for **PEGalk-A1** hydrogel preparation for each polymer concentration (see Supporting Information, Table S1).

Inverted Vial Test. Hydrogels were prepared as stated above. The timer was started immediately after the addition of the amine solution and vortex mixing. Gelation time was determined when no flow was observed after inverting the vial. The experiments were carried out in triplicate, so gelation times were presented as an average.

Rheological Analysis. Rheological measurements were performed on a HAAKE MARS 40 rheometer with a parallel plate measuring system and a gap of 0.5 mm. The lower plate was heated to the desired temperature. Then, the precursor solutions of hydrogels were prepared separately so that they were pipetted onto the plate, mixed *in situ*, and the measurement started immediately after.

EWC. The EWC index was studied to characterize the water content of the hydrogel in a steady state. In order to be measured, free hydrogels were removed from the reaction vials, frozen in liquid nitrogen, and lyophilized for 24 h. Freeze-dried hydrogels were weighted (dried mass, W_d) and immersed in pH = 7.4 buffer. Swelling was monitored by a weighting method, where the hydrogels were allowed to swell and their weight was recorded over time (W_t), calculating their swelling ratio at each time as follows:

$$\text{Swelling Ratio} = \frac{W_t - W_d}{W_d} \times 100\%$$

All measurements were repeated in triplicate. Swelling equilibrium is considered to be reached once W_t stays constant over time (W_f), so that EWC is calculated as follows:

$$\text{EWC} = \frac{W_f - W_d}{W_f} \times 100\%$$

Hydrogel Morphology. The microstructure of the gel was visualized by SEM. The hydrogel was prepared as stated above, in a 4 mL vial at 10, 20, or 30 wt % polymer concentration in a final mass of 200 mg. Then, the recovered hydrogel was immersed in pH 7.4 buffer for 1 h, frozen in liquid nitrogen, and subsequently snapped to expose the cross-section. After being lyophilized, the xerogel was coated with Pt for observation under SEM.

MIP. MIP was performed using a Micromeritics AutoPore IV 9500 porosimeter to determine macro- and mesoporosity and pore size distribution. Between 2 and 3 replicas were evaluated to ensure accurate results. The pore diameter distribution curves were calculated using the Washburn equation:

$$pd = -4\Upsilon\cos\vartheta$$

where p is the pressure required to force mercury into the pores, d is the diameter of the pores, Υ is the mercury surface tension (485 dyn cm^{-1}), and ϑ is the contact angle between mercury and the sample.

^{1}H-HR-MAS NMR Spectroscopy. All HR-MAS NMR spectra were acquired at room temperature on a Bruker Avance NEO 400 spectrometer operating at a proton Larmor frequency of 400.13 MHz and equipped with a 4 mm double-resonance (1H, 13C) gradient HR-MAS probe. Samples were prepared in a pH 7.4 buffer and swollen with a drop of deuterium oxide in the probe. Chemical shifts were referenced to the TMSP (as an internal reference). The gels were mechanically stable at the moderate MAS rate of 4 kHz used in all the HR-MAS experiments, and no sample instabilities resulting from centrifugation-related phenomena were detected.

Hydrogel pH-Induced Degradation. Free hydrogels were removed from the reaction vials, so the material was able to be weighted (W_0) and immersed in 2 mL of aqueous solution of the appropriate pH (7.4, 5.0 or 2.0) at 25 °C. Swelling/degradation was monitored by a weighting method, where the hydrogels were allowed to swell, and their weight was recorded at appropriate time points (W_t). The aqueous solution of the appropriate pH was renewed every 24 h. All measurements were repeated in triplicate. Results are represented as a function of the relative weight at each time (mean ± SD (n = 3)):

$$\text{Relative Weight} = \frac{W_t}{W_0}$$

Hydrogel Temperature-Induced Degradation. Process is performed identically as stated above, immersing hydrogels in 2 mL of pH 7.4 buffer at the desired temperature (25 or 37 °C).

■ ASSOCIATED CONTENT

Supporting Information

The Supporting Information is available free of charge at https://pubs.acs.org/doi/10.1021/acs.macromol.4c01403.

Additional characterization data including NMR, FTIR, ESI HRMS, MALDI-ToF MS, DSC, rheology, and MIP results (PDF)

■ AUTHOR INFORMATION

Corresponding Authors

Milagros Piñol − *Instituto de Nanociencia y Materiales de Aragón (INMA), CSIC-Universidad de Zaragoza, Zaragoza 50009, Spain; Departamento de Química Orgánica, Facultad de Ciencias, Universidad de Zaragoza, Zaragoza 50009, Spain*; Email: mpinol@unizar.es

Luis Oriol − *Instituto de Nanociencia y Materiales de Aragón (INMA), CSIC-Universidad de Zaragoza, Zaragoza 50009, Spain; Departamento de Química Orgánica, Facultad de Ciencias, Universidad de Zaragoza, Zaragoza 50009, Spain;* orcid.org/0000-0002-0922-5615; Email: loriol@unizar.es

Authors

Sara Bescós-Ramo − *Instituto de Nanociencia y Materiales de Aragón (INMA), CSIC-Universidad de Zaragoza, Zaragoza 50009, Spain; Departamento de Química Orgánica, Facultad de Ciencias, Universidad de Zaragoza, Zaragoza 50009, Spain;* orcid.org/0009-0008-6456-4856

Jesús del Barrio − *Instituto de Nanociencia y Materiales de Aragón (INMA), CSIC-Universidad de Zaragoza, Zaragoza 50009, Spain;* orcid.org/0000-0002-5380-6863

Pilar Romero − *Instituto de Nanociencia y Materiales de Aragón (INMA), CSIC-Universidad de Zaragoza, Zaragoza 50009, Spain; Departamento de Química Orgánica, Facultad de Ciencias, Universidad de Zaragoza, Zaragoza 50009, Spain;* orcid.org/0000-0003-1378-0571

Laura Florentino-Madiedo − *Instituto de Nanociencia y Materiales de Aragón (INMA), CSIC-Universidad de Zaragoza, Zaragoza 50009, Spain; Departamento de Ingeniería Química y Tecnologías del Medio Ambiente, Universidad de Zaragoza, Zaragoza 50018, Spain*

Complete contact information is available at: https://pubs.acs.org/10.1021/acs.macromol.4c01403

Notes

The authors declare no competing financial interest.

■ ACKNOWLEDGMENTS

This work was financially supported by Ministerio de Ciencia e Innovación (PID2021-126132NB-I00), the Grant CEX2023-001286-S funded by MICIU/AEI/10.13039/501100011033, and Gobierno de Aragón-FSE (E47_23R research group). S.B-R. acknowledges Gobierno de Aragón for her Ph.D. grant. The

authors would like to acknowledge the use of Laboratorio de Microscopias Avanzadas-LMA (Instituto de Nanociencia y Materiales de Aragón-Universidad de Zaragoza), Servicio General de Apoyo a la Investigación-SAI (Universidad de Zaragoza), and Servicios Científico-Técnicos of CEQMA (CSIC-Universidad de Zaragoza) and Conexión Nanomedicina (CSIC).

REFERENCES

(1) Zhang, Y. S.; Khademhosseini, A. Advances in Engineering Hydrogels. *Science* **2017**, *356* (6337), No. eaaf3627.
(2) Liang, Y.; He, J.; Guo, B. Functional Hydrogels as Wound Dressing to Enhance Wound Healing. *ACS Nano* **2021**, *15* (8), 12687−12722.
(3) Qi, L.; Zhang, C.; Wang, B.; Yin, J.; Yan, S. Progress in Hydrogels for Skin Wound Repair. *Macromol. Biosci.* **2022**, *22* (7), 2100475.
(4) Li, J.; Mooney, D. J. Designing Hydrogels for Controlled Drug Delivery. *Nat. Rev. Mater.* **2016**, *1* (12), 16071.
(5) Harris, J. M.; Chess, R. B. Effect of Pegylation on Pharmaceuticals. *Nat. Rev. Drug Discov* **2003**, *2* (3), 214−221.
(6) Hu, W.; Wang, Z.; Xiao, Y.; Zhang, S.; Wang, J. Advances in Crosslinking Strategies of Biomedical Hydrogels. *Biomater. Sci.* **2019**, *7* (3), 843−855.
(7) DeForest, C. A.; Polizzotti, B. D.; Anseth, K. S. Sequential Click Reactions for Synthesizing and Patterning Three-Dimensional Cell Microenvironments. *Nat. Mater.* **2009**, *8* (8), 659−664.
(8) DeForest, C. A.; Sims, E. A.; Anseth, K. S. Peptide-Functionalized Click Hydrogels with Independently Tunable Mechanics and Chemical Functionality for 3D Cell Culture. *Chem. Mater.* **2010**, *22* (16), 4783−4790.
(9) Zheng, J.; Smith Callahan, L. A.; Hao, J.; Guo, K.; Wesdemiotis, C.; Weiss, R. A.; Becker, M. L. Strain-Promoted Cross-Linking of PEG-Based Hydrogels via Copper-Free Cycloaddition. *ACS Macro Lett.* **2012**, *1* (8), 1071−1073.
(10) Truong, V. X.; Ablett, M. P.; Gilbert, H. T. J.; Bowen, J.; Richardson, S. M.; Hoyland, J. A.; Dove, A. P. In Situ-Forming Robust Chitosan-Poly(Ethylene Glycol) Hydrogels Prepared by Copper-Free Azide−Alkyne Click Reaction for Tissue Engineering. *Biomater. Sci.* **2014**, *2* (2), 167−175.
(11) Ono, R. J.; Lee, A. L. Z.; Voo, Z. X.; Venkataraman, S.; Koh, B. W.; Yang, Y. Y.; Hedrick, J. L. Biodegradable Strain-Promoted Click Hydrogels for Encapsulation of Drug-Loaded Nanoparticles and Sustained Release of Therapeutics. *Biomacromolecules* **2017**, *18* (8), 2277−2285.
(12) Fu, S.; Dong, H.; Deng, X.; Zhuo, R.; Zhong, Z. Injectable Hyaluronic Acid/Poly(Ethylene Glycol) Hydrogels Crosslinked *via* Strain-Promoted Azide-Alkyne Cycloaddition Click Reaction. *Carbohydr. Polym.* **2017**, *169*, 332−340.
(13) Lagneau, N.; Tournier, P.; Halgand, B.; Loll, F.; Maugars, Y.; Guicheux, J.; Le Visage, C.; Delplace, V. Click and Bioorthogonal Hyaluronic Acid Hydrogels as an Ultra-Tunable Platform for the Investigation of Cell-Material Interactions. *Bioact. Mater.* **2023**, *24*, 438−449.
(14) van de Wetering, P.; Metters, A. T.; Schoenmakers, R. G.; Hubbell, J. A. Poly(Ethylene Glycol) Hydrogels Formed by Conjugate Addition with Controllable Swelling, Degradation, and Release of Pharmaceutically Active Proteins. *J. Controlled Release* **2005**, *102* (3), 619−627.
(15) Rydholm, A. E.; Reddy, S. K.; Anseth, K. S.; Bowman, C. N. Development and Characterization of Degradable Thiol-Allyl Ether Photopolymers. *Polymer* **2007**, *48* (15), 4589−4600.
(16) Kharkar, P. M.; Kloxin, A. M.; Kiick, K. L. Dually Degradable Click Hydrogels for Controlled Degradation and Protein Release. *J. Mater. Chem. B* **2014**, *2* (34), 5511−5521.
(17) Kharkar, P. M.; Rehmann, M. S.; Skeens, K. M.; Maverakis, E.; Kloxin, A. M. Thiol−Ene Click Hydrogels for Therapeutic Delivery. *ACS Biomater. Sci. Eng.* **2016**, *2* (2), 165−179.
(18) Alge, D. L.; Azagarsamy, M. A.; Donohue, D. F.; Anseth, K. S. Synthetically Tractable Click Hydrogels for Three-Dimensional Cell Culture Formed Using Tetrazine−Norbornene Chemistry. *Biomacromolecules* **2013**, *14* (4), 949−953.
(19) Guaresti, O.; García−Astrain, C.; Aguirresarobe, R. H.; Eceiza, A.; Gabilondo, N. Synthesis of Stimuli−Responsive Chitosan−Based Hydrogels by Diels−Alder Cross−Linking̀ click′ Reaction as Potential Carriers for Drug Administration. *Carbohydr. Polym.* **2018**, *183*, 278−286.
(20) Zander, Z. K.; Hua, G.; Wiener, C. G.; Vogt, B. D.; Becker, M. L. Control of Mesh Size and Modulus by Kinetically Dependent Cross-Linking in Hydrogels. *Adv. Mater.* **2015**, *27* (40), 6283−6288.
(21) Grover, G. N.; Lam, J.; Nguyen, T. H.; Segura, T.; Maynard, H. D. Biocompatible Hydrogels by Oxime Click Chemistry. *Biomacromolecules* **2012**, *13* (10), 3013−3017.
(22) Grover, G. N.; Braden, R. L.; Christman, K. L. Oxime Cross-Linked Injectable Hydrogels for Catheter Delivery. *Adv. Mater.* **2013**, *25* (21), 2937−2942.
(23) Lin, F.; Yu, J.; Tang, W.; Zheng, J.; Defante, A.; Guo, K.; Wesdemiotis, C.; Becker, M. L. Peptide-Functionalized Oxime Hydrogels with Tunable Mechanical Properties and Gelation Behavior. *Biomacromolecules* **2013**, *14* (10), 3749−3758.
(24) Truong, V. X.; Ablett, M. P.; Richardson, S. M.; Hoyland, J. A.; Dove, A. P. Simultaneous Orthogonal Dual-Click Approach to Tough, in-Situ-Forming Hydrogels for Cell Encapsulation. *J. Am. Chem. Soc.* **2015**, *137* (4), 1618−1622.
(25) Cai, X. Y.; Li, J. Z.; Li, N. N.; Chen, J. C.; Kang, E.-T.; Xu, L. Q. PEG-Based Hydrogels Prepared by Catalyst-Free Thiol−Yne Addition and Their Post-Antibacterial Modification. *Biomater. Sci.* **2016**, *4* (11), 1663−1672.
(26) Macdougall, L. J.; Truong, V. X.; Dove, A. P. Efficient In Situ Nucleophilic Thiol-Yne Click Chemistry for the Synthesis of Strong Hydrogel Materials with Tunable Properties. *ACS Macro Lett.* **2017**, *6* (2), 93−97.
(27) Fan, B.; Zhang, K.; Liu, Q.; Eelkema, R. Self-Healing Injectable Polymer Hydrogel via Dynamic Thiol-Alkynone Double Addition Cross-Links. *ACS Macro Lett.* **2020**, *9* (6), 776−780.
(28) Worch, J. C.; Stubbs, C. J.; Price, M. J.; Dove, A. P. Click Nucleophilic Conjugate Additions to Activated Alkynes: Exploring Thiol-Yne, Amino-Yne, and Hydroxyl-Yne Reactions from (Bio)-Organic to Polymer Chemistry. *Chem. Rev.* **2021**, *121* (12), 6744−6776.
(29) Yang, R.; Zhang, X.; Chen, B.; Yan, Q.; Yin, J.; Luan, S. Tunable Backbone-Degradable Robust Tissue Adhesives via in Situ Radical Ring-Opening Polymerization. *Nat. Commun.* **2023**, *14* (1), 6063.
(30) Burek, M.; Waśkiewicz, S.; Lalik, A.; Wandzik, I. Hydrogels with Novel Hydrolytically Labile Trehalose-Based Crosslinks: Small Changes − Big Differences in Degradation Behavior. *Polym. Chem.* **2018**, *9* (27), 3721−3726.
(31) Feng, X.; Du, M.; Wei, H.; Ruan, X.; Fu, T.; Zhang, J.; Sun, X. Chemically Triggered Life Control of "Smart" Hydrogels through Click and Declick Reactions. *Front. Chem. Sci. Eng.* **2022**, *16* (9), 1399−1406.
(32) Schneider, E. L.; Henise, J.; Reid, R.; Ashley, G. W.; Santi, D. V. Hydrogel Drug Delivery System Using Self-Cleaving Covalent Linkers for Once-a-Week Administration of Exenatide. *Bioconjugate Chem.* **2016**, *27* (5), 1210−1215.
(33) Du, M.; Jin, J.; Zhou, F.; Chen, J.; Jiang, W. Dual Drug-Loaded Hydrogels with pH-Responsive and Antibacterial Activity for Skin Wound Dressing. *Colloids Surf. B Biointerfaces* **2023**, *222*, No. 113063.
(34) Zhu, C.; Zhao, J.; Kempe, K.; Wilson, P.; Wang, J.; Velkov, T.; Li, J.; Davis, T. P.; Whittaker, M. R.; Haddleton, D. M. A Hydrogel-Based Localized Release of Colistin for Antimicrobial Treatment of Burn Wound Infection. *Macromol. Biosci.* **2017**, *17* (2), 1600320.
(35) Yang, H.; Fustin, C.-A. Design and Applications of Dynamic Hydrogels Based on Reversible C═N Bonds. *Macromol. Chem. Phys.* **2023**, *224* (20), 2300211.
(36) Zhang, X.; Malhotra, S.; Molina, M.; Haag, R. Micro- and Nanogels with Labile Crosslinks − from Synthesis to Biomedical Applications. *Chem. Soc. Rev.* **2015**, *44* (7), 1948−1973.

https://doi.org/10.1021/acs.macromol.4c01403
Macromolecules 2024, 57, 10926−10937

(37) He, B.; Su, H.; Bai, T.; Wu, Y.; Li, S.; Gao, M.; Hu, R.; Zhao, Z.; Qin, A.; Ling, J.; Tang, B. Z. Spontaneous Amino-Yne Click Polymerization: A Powerful Tool toward Regio- and Stereospecific Poly(β-Aminoacrylate)s. *J. Am. Chem. Soc.* **2017**, *139* (15), 5437−5443.
(38) Zhang, J.; Zhang, Z.; Wang, J.; Zang, Q.; Sun, J. Z.; Tang, B. Z. Recent Progress in the Applications of Amino−Yne Click Chemistry. *Polym. Chem.* **2021**, *12* (20), 2978−2986.
(39) Li, D.; Song, Y.; He, J.; Zhang, M.; Ni, P. Polymer−Doxorubicin Prodrug with Biocompatibility, pH Response, and Main Chain Breakability Prepared by Catalyst-Free Click Reaction. *ACS Biomater. Sci. Eng.* **2019**, *5* (5), 2307−2315.
(40) Chi, T.; Sang, T.; Wang, Y.; Ye, Z. Cleavage and Noncleavage Chemistry in Reactive Oxygen Species (ROS)-Responsive Materials for Smart Drug Delivery. *Bioconjugate Chem.* **2024**, *35* (1), 1−21.
(41) Fenton, O. S.; Andresen, J. L.; Paolini, M.; Langer, R. β-Aminoacrylate Synthetic Hydrogels: Easily Accessible and Operationally Simple Biomaterials Networks. *Angew. Chem., Int. Ed.* **2018**, *57* (49), 16026−16029.
(42) Huang, J.; Jiang, X. Injectable and Degradable pH-Responsive Hydrogels via Spontaneous Amino−Yne Click Reaction. *ACS Appl. Mater. Interfaces* **2018**, *10* (1), 361−370.
(43) Li, H.-C.; Sun, X.-M.; Huang, Y.-R.; Peng, Y.-H.; Liu, J.; Ren, L. Synthetic Crosslinker Based on Amino−Yne Click to Enhance the Suture Tension of Collagen-Based Corneal Repair Materials. *ACS Appl. Polym. Mater.* **2022**, *4* (6), 4495−4507.
(44) Oktay, B.; Demir, S.; Kayaman-Apohan, N. Immobilization of Pectinase on Polyethyleneimine Based Support via Spontaneous Amino-Yne Click Reaction. *Food Bioprod. Process.* **2020**, *122*, 159−168.
(45) Zhang, R.; Tian, Y.; Pang, L.; Xu, T.; Yu, B.; Cong, H.; Shen, Y. Wound Microenvironment-Responsive Protein Hydrogel Drug-Loaded System with Accelerating Healing and Antibacterial Property. *ACS Appl. Mater. Interfaces* **2022**, *14* (8), 10187−10199.
(46) Deng, M.; Wu, Y.; Ren, Y.; Song, H.; Zheng, L.; Lin, G.; Wen, X.; Tao, Y.; Kong, Q.; Wang, Y. Clickable and Smart Drug Delivery Vehicles Accelerate the Healing of Infected Diabetic Wounds. *J. Controlled Release* **2022**, *350*, 613−629.
(47) Li, Q.; Hu, Z.; Ji, X. Hydrogel-Based Macroscopic Click Chemistry. *Angew. Chem., Int. Ed.* **2023**, *62* (52), No. e202315086.
(48) Nguyen, C. T. V.; Chow, S. K. K.; Nguyen, H. N.; Liu, T.; Walls, A.; Withey, S.; Liebig, P.; Mueller, M.; Thierry, B.; Yang, C.-T.; Huang, C.-J. Formation of Zwitterionic and Self-Healable Hydrogels via Amino-Yne Click Chemistry for Development of Cellular Scaffold and Tumor Spheroid Phantom for MRI. *ACS Appl. Mater. Interfaces* **2024**, *16* (28), 36157−36167.
(49) Paula, C. T. B.; Pereira, P.; Coelho, J. F. J.; Fonseca, A. C.; Serra, A. C. Development of Light-Degradable Poly(Urethane-Urea) Hydrogel Films. *Mater. Sci. Eng. C Mater. Biol. Appl.* **2021**, *131*, No. 112520.
(50) Paula, C. T. B.; Leandro, A.; Pereira, P.; Coelho, J. F. J.; Fonseca, A. C.; Serra, A. C. Fast-Gelling Polyethylene Glycol/Polyethyleneimine Hydrogels Degradable by Visible-Light. *Macromol. Biosci.* **2024**, *24* (2), 2300289.
(51) Kharkar, P. M.; Kiick, K. L.; Kloxin, A. M. Designing Degradable Hydrogels for Orthogonal Control of Cell Microenvironments. *Chem. Soc. Rev.* **2013**, *42* (17), 7335−7372.
(52) He, B.; Zhang, J.; Wang, J.; Wu, Y.; Qin, A.; Tang, B. Z. Preparation of Multifunctional Hyperbranched Poly(β-Aminoacrylate)s by Spontaneous Amino-Yne Click Polymerization. *Macromolecules* **2020**, *53* (13), 5248−5254.
(53) Wang, D.; Zhang, N.; Yang, T.; Jing, X.; Meng, L. Construction Polyprodrugs by Click-Reactions and Metal-Coordination: pH-Responsive Release for Magnetic Resonance Imaging Guided Chemotherapy. *Chem. Eng. J.* **2021**, *422*, No. 130108.
(54) Gonzaga, F.; Grande, J. B.; Brook, M. A. Morphology-Controlled Synthesis of Poly(Oxyethylene)Silicone or Alkylsilicone Surfactants with Explicit, Atomically Defined, Branched, Hydrophobic Tails. *Chem. - Eur. J.* **2012**, *18* (5), 1536−1541.
(55) Abdel-Khalik, M. M.; Elnagdi, M. H. Enaminones in Organic Synthesis: A Novel Synthesis of 1,3,5-Trisubstituted Benzene Derivatives and of 2-Substituted-5-Aroylpyridines. *Synth. Commun.* **2002**, *32* (2), 159−164.
(56) Wan, J.-P.; Lin, Y.; Hu, K.; Liu, Y. Metal-Free Synthesis of 1,3,5-Trisubstituted Benzenes by the Cyclotrimerization of Enaminones or Alkynes in Water. *RSC Adv.* **2014**, *4* (39), 20499−20505.
(57) Elghamry, I. Cyclotrimerization of Enaminones: An Efficient Method for the Synthesis of 1,3,5-Triaroylbenzenes. *Synthesis* **2003**, *35* (15), 2301.
(58) Park, H.; Guo, X.; Temenoff, J. S.; Tabata, Y.; Caplan, A. I.; Kasper, F. K.; Mikos, A. G. Effect of Swelling Ratio of Injectable Hydrogel Composites on Chondrogenic Differentiation of Encapsulated Rabbit Marrow Mesenchymal Stem Cells In Vitro. *Biomacromolecules* **2009**, *10* (3), 541−546.
(59) Ferreira, L.; Gil, M. H.; Dordick, J. S. Enzymatic Synthesis of Dextran-Containing Hydrogels. *Biomaterials* **2002**, *23* (19), 3957−3967.
(60) Camci-Unal, G.; Cuttica, D.; Annabi, N.; Demarchi, D.; Khademhosseini, A. Synthesis and Characterization of Hybrid Hyaluronic Acid-Gelatin Hydrogels. *Biomacromolecules* **2013**, *14* (4), 1085−1092.
(61) Peppas, N. A.; Moynihan, H. J.; Lucht, L. M. The structure of highly crosslinked poly(2-hydroxyethyl methacrylate) hydrogels. *J. Biomed. Mater. Res.* **1985**, *19* (4), 397−411.
(62) Muralidharan, A.; McLeod, R. R.; Bryant, S. J. Hydrolytically Degradable Poly(β-Amino Ester) Resins with Tunable Degradation for 3D Printing by Projection Micro-Stereolithography. *Adv. Funct. Mater.* **2022**, *32* (6), 2106509.

https://doi.org/10.1021/acs.macromol.4c01403
Macromolecules 2024, 57, 10926−10937